Proc. Natl. Acad. Sci. USA
Vol. 88, pp. 4661–4665, June 1991
Chemistry

Kinetics of antigenic peptide binding to the class II major histocompatibility molecule I-A^d

(reaction mechanism/antigen presentation)

ROBERT TAMPÉ AND HARDEN M. MCCONNELL*

Stauffer Laboratory for Physical Chemistry, Stanford University, Stanford, CA 94305

Contributed by Harden M. McConnell, February 27, 1991

ABSTRACT **Using high-performance size-exclusion chromatography and fluorescence spectroscopy, we investigated the kinetics of fluorescent peptide reactions with detergent-solubilized I-A^d, a class II molecule of the mouse major histocompatibility complex. At pH 7.0 and 37°C the half-time for the binding of a fluorescein-labeled synthetic peptide representing ovalbumin amino acids 323–339 [FOva-(323–339)Y] to I-A^d was 32 hr, independent of added fluorescent peptide concentration in the range 5–200 μM. Peptide exchange experiments were also carried out, where it was found that the half-time of FOva-(323–339)Y binding was equal to the half-time of dissociation of the Texas Red-labeled peptide TROva-(323–339)Y. These experiments show that slow peptide binding to class II major histocompatibility molecules may be limited by the slow dissociation of prebound peptides. Paradoxically, however, this kinetic behavior—a peptide concentration-insensitive on-reaction with a half-time for peptide binding approximately equal to the half-time for dissociation—can be modeled in more than one way. Models involving a kinetic intermediate are particularly attractive. The kinetics were significantly different at pH 5.0. The half-times for peptide binding and dissociation were ≈7 times shorter than at pH 7.0. In addition the complex of the I-A^d α/β heterodimer with FOva-(323–339)Y was unstable and dissociated into separate α and β chains with a half-time of ≈7 hr.**

The immune recognition by T helper cells involves many different steps, including antigen internalization by endocytosis and endosomal processing in acidic cell compartments. This leads to fragmentation of the protein to peptides. Some of these antigenic peptides bind to class II molecules of the major histocompatibility complex (MHC) and are transported to the cell surface. These MHC–peptide complexes "present" the antigenic peptide to CD4$^+$ T cells (for review see refs. 1 and 2). Thus, the recognition process by T helper cells requires antigen processing and subsequent presentation on the cell surface by MHC class II molecules. The recognition event causes activation of the immune system, a complex series of events involving humoral messengers. Peptide binding to MHC class II molecules is thus a central step in immune recognition. It is not known, however, by what molecular mechanism MHC molecules bind peptide. There are indications that MHC class II molecules are recycled from the cell surface by endocytosis (3). Acidification of the endosomal compartment presumably allows peptide release and rebinding of new peptides. On the molecular level, the kinetics of peptide association and dissociation have been investigated in both detergent solution and planar membranes (4–8). Once formed, the MHC–peptide complex is long-lived and dissociates with a half-life of several days (6–8). A long-lived complex is doubtless essential for its function in cell–cell recognition and triggering.

The interpretation of the kinetics of peptide binding is not straightforward. A number of reports assume that the reaction is a slow, second-order, single-step reaction (6, 7). However, Sadegh-Nasseri and McConnell (8) obtained evidence that peptide binding with the mouse MHC class II molecule I-E^k is not a single-step reaction.

In the present work we have investigated peptide binding, dissociation, and exchange with the mouse class II molecule I-A^d in detergent solution by high-performance size-exclusion chromatography (HPSEC). Using peptides labeled with different fluorescent tags, we followed the peptide exchange at different pH values. Our results appear to be consistent with a kinetic intermediate of the sort proposed earlier (8) but reveal in addition an unexpected finding that the half-time for peptide binding to I-A^d is equal to the half-time for peptide dissociation, over a wide range of added peptide concentrations. In related work in this laboratory the same result has been obtained for pigeon cytochrome *c* peptide binding to I-E^k (S. Witt and H.M.M., unpublished data).

METHODS

Cell Lines and Materials. As a source of I-A^d we used the cell line A20.1.11 (9). I-A^d was purified by affinity chromatography using the monoclonal antibody MKD6 (anti-I-A^d). After periodate oxidation the MKD6 antibody was coupled to hydrazine-agarose (Bio-Rad). Both cell lines were obtained from the American Type Culture Collection.

Purification of I-A^d. A20.1.11 cells were grown in RPMI 1640 medium (GIBCO) supplemented with 10% NuSerum IV (Collaborative Research), 2 mM glutamine (GIBCO), and 1 mM sodium pyruvate (GIBCO). Viability of the cells was >95%. Cells were harvested and washed twice with phosphate-buffered isotonic saline containing (PBS) 1 mM $CaCl_2$ and 1 mM $MgCl_2$ (pH 7.3). For lysis, cells were suspended at 4°C in 0.5% Nonidet P-40 (Sigma)/10 mM Tris·HCl/150 mM NaCl/0.001% aprotinin (20 trypsin inhibitory units/mg; Sigma)/1 mM phenylmethylsulfonyl fluoride (Sigma)/0.25 mM thimerosal (Sigma), pH 8.3. The lysate was centrifugated at 1200 × *g* (30 min) and at 100,000 × *g* (60 min). The centrifugate was applied to a lentil lectin column (Pharmacia) equilibrated in lysis buffer. Glycoproteins were eluted in 10% methyl α-D-mannoside (Sigma) and directly applied to the MKD6 antibody column. The detergent was exchanged with 1 mM dodecyl β-D-maltoside (DM; Calbiochem) in PBS (pH

The publication costs of this article were defrayed in part by page charge payment. This article must therefore be hereby marked "*advertisement*" in accordance with 18 U.S.C. §1734 solely to indicate this fact.

Abbreviations: MHC, major histocompatibility complex; Ova-(323–339)Y, synthetic peptide representing amino acids 323–339 of chicken ovalbumin plus a C-terminal tyrosine; FOva-(323–339)Y, fluorescein-labeled (N terminus) Ova-(323–339)Y; TROva-(323–339)Y; Texas Red-labeled (N terminus) Ova(323–339)Y; HSV-(8–23), synthetic peptide representing amino acids 8–23 of herpes simplex virus glycoprotein D; DM, dodecyl β-D-maltoside; HPSEC, high-performance size-exclusion chromatography.

*To whom reprint requests should be addressed.

7.0). The bound IA^d was eluted with 1 mM DM/50 mM $NaHCO_3$/0.5 M NaCl/0.02% NaN_3, pH 11.0. The elution of protein was monitored spectroscopically at 280 nm. The eluate was immediately neutralized, concentrated, and dialyzed in the HPSEC running buffer. The preparation was characterized by protein determination and SDS/PAGE.

Peptides. Peptides representing ovalbumin (Ova) amino acids 323–339 [Ova-(323–339)Y, where Y is an added C-terminal tyrosine] and 323–328 [Ova-(323–328)] were synthesized by the solid-phase technique on a Milligen 9050 peptide synthesizer. After purification by HPLC using a preparative C_{18} reverse-phase column (Vydac; The Separations Group), peptides were labeled at the N terminus with fluorescein isothiocyanate (Molecular Probes) or Texas Red sulfonyl chloride (Molecular Probes), to give FOva or TROva peptides, respectively. The reaction was carried out in dimethyl sulfoxide in the presence of an organic base. The reaction was monitored by HPLC using an analytical C_{18} reverse-phase column (Vydac). The labeled peptides were precipitated by addition of ethyl acetate and purified using a preparative C_{18} reverse-phase column. Control and competition experiments were carried out with the peptide HSV-(8–23), which represents amino acids 8–23 of the herpes simplex virus glycoprotein D and was kindly provided by B. R. Clark (Biospan, Redwood City, CA).

Analytical SDS/PAGE. $I\text{-}A^d$ samples (0.3 μM in 10 mM citrate/phosphate buffer, pH 7–4/150 mM NaCl/0.02% NaN_3) were incubated with 100 μM FOva-(323–339)Y at 37°C for 5 days. Aliquots (20 μl) were applied to an SDS/12.5% polyacrylamide gel under nonreducing conditions. The gels were silver-stained (10). The relative amounts of $I\text{-}A^d$ α chain, β chain, and α/β heterodimer were determined using the LKB UltroScan XL laser scanner. The scans were corrected for background. The amount of FOva peptide bound to $I\text{-}A^d$ was determined by HPSEC.

HPSEC. HPSEC was performed using a Rainin-HPX solvent delivery system with pressure monitor. The column (Ultropac TSK G3000 SW, 7.5 × 600 mm, Pharmacia) and precolumn (Ultropac TSK SWP, 7.5 × 75 mm, Pharmacia) were connected to an absorbance detector (Kratos Analytical Instruments) and a fluorometer (Gilson model 121). The elution of FOva peptide was followed using a narrow excitation filter (490 nm) and a narrow emission filter (520 nm). For the detection of TROva peptide, we used a narrow filter (570 nm) and a wide-range, colored glass filter (585–650 nm). HPSEC separations were performed in 1 mM DM/10 mM phosphate buffer/150 mM NaCl/0.02% NaN_3, pH 7.0. The flow rate was 1 ml/min. The amount of peptide injected into the HPSEC was checked by the absorbance detector at 280 nm. We used an injection volume of 20 or 200 μl. For separate measurements the elution fractions were collected and analyzed by SDS/PAGE and fluorescence spectroscopy.

Fluorescence Spectroscopy. To determine the relative concentration of FOva and TROva peptides in an elution fraction we used a Spex Fluorolog fluorometer. FOva and TROva peptides were excited at 475 and 575 nm, respectively. Emission spectra were recorded from 500–700 nm and 600–700 nm, respectively. The fluorescence intensities at 520 nm (FOva) and 610 nm (TROva) were corrected for background and normalized to zero and unity.

RESULTS

Kinetics of Peptide–MHC Association. The TSK G3000 SW size-exclusion column enabled us to separate $I\text{-}A^d$ from a large excess of free peptide. The $I\text{-}A^d$ heterodimer and free peptide were eluted at 15 ml and 25 ml, respectively. Samples of detergent-solubilized $I\text{-}A^d$ were incubated with various concentrations of FOva-(323–339)Y at 37°C. The samples had the final composition 0.3 μM $I\text{-}A^d$/5–200 μM FOva-(323–339)Y/1 mM DM/10 mM phosphate or acetate buffer, pH 7.0 or pH 5.0)/150 mM NaCl/0.02% NaN_3. Fig. 1*A* displays the ratio of bound peptide to $I\text{-}A^d$ over a period of 3 days. All binding curves show a very slow binding. For different peptide concentrations the curves reach a different equilibrium level. After 10 days the amount of bound peptide was determined as a function of the peptide concentration (Fig. 1*B*). The amount of bound FOva peptide increased asymptotically with the peptide concentration. With the assumption that the reaction reached equilibrium, the data were analyzed by a Scatchard plot. The apparent dissociation constant, K_d, was determined to be 28 μM. The maximum amount of bound peptide was 0.75%. Analyzing the association data as a pseudo-first-order reaction, Fig. 1*C* gives $\ln\{[MP]_{eq}/([MP]_{eq} - [MP])\}$ as a function of time. The pseudo-first-order rate constant, k, is independent of the peptide concentration: $k = 1.1 \times 10^{-5}$, 1.6×10^{-5}, and 1.5×10^{-5} s^{-1}, respectively, at 100, 50, and 5 μM FOva-(323–339)Y. The binding specificity of Ova peptide was checked using the HSV-(8–23) peptide. After incubation for several days, binding to $I\text{-}A^d$ could not be detected. In general, 100 μM HSV (8–23) did not compete with the binding of FOva peptide.

Dissociation Kinetics. $I\text{-}A^d$ was incubated with a large excess of FOva-(323–339)Y in detergent solution at 37°C. After 10 days the $I\text{-}A^d$ heterodimer was isolated by HPSEC. Monitor-

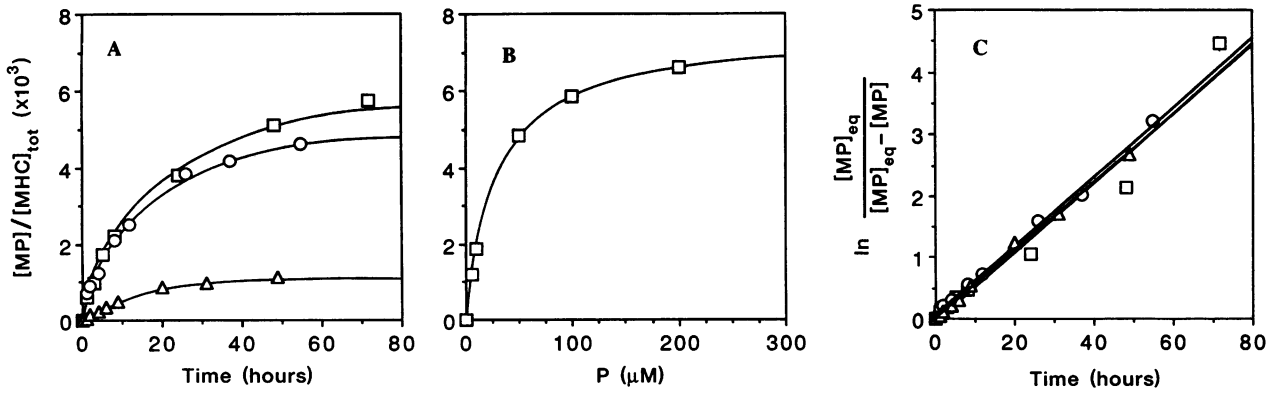

FIG. 1. Binding of FOva-(323–339)Y to $I\text{-}A^d$. Samples containing 0.3 μM $I\text{-}A^d$ were incubated with various concentrations of peptide (5–200 μM) at 37°C in 1 mM DM/10 mM phosphate buffer, pH 7.0/150 mM NaCl/0.02% NaN_3. At certain times small sample volumes were analyzed by HPSEC. At the size-exclusion volume of the heterodimer, peptide binding was analyzed by the fluorescence intensity. Using fluorescent peptide concentrations as standards we determined the absolute amount of bound peptide, $[MP]/[MHC]_{tot}$. (*A*) Association of FOva-(323–339)Y as a function of time for different peptide concentrations: 5 μM (△), 50 μM (○), and 100 μM (□). (*B*) Association of FOva-(323–339)Y after 10 days as a function of the total amount of peptide (P). (*C*) Assuming a first-order association reaction, we plot $\ln\{[MP]_{eq}/([MP]_{eq} - [MP])\}$ versus time, where $[MP]_{eq}$ is the equilibrium concentration of bound peptide. Total peptide concentrations: 5 μM (△), 50 μM (○), and 100 μM (□).

ing of peptide dissociation at 37°C was started immediately by addition of unlabeled or differently labeled Ova(323–339)Y to a final concentration of 0.1 mM in 0.3 μM I-A^d/1 mM DM/10 mM phosphate or acetate buffer, pH 7.0 or 5.0/150 mM NaCl/0.02% NaN_3. At various times small samples were analyzed by HPSEC. The dissociation of the MHC–peptide complex corresponded to a first-order dissociation with $k = 6.0 \times 10^{-6}\ s^{-1}$ (Fig. 2). The dissociation rate was comparable to the rate found for the binding of the Ova peptide to I-A^d. The dissociation rate was not altered in the presence of different detergents such as octyl β-D-glucopyranoside, SDS, or deoxycholate. At pH 5.0 we found a 7-fold increase of the dissociation rate ($k = 4.2 \times 10^{-5}\ s^{-1}$). The dissociation rate was studied for two differently labeled Ova peptides (FOva and TROva). The dissociation rate was independent of the fluorescent dye used for peptide labeling and was not altered when the dissociation took place in the presence of an excess of unlabeled or differently labeled peptide.

Peptide Exchange. Using two differently labeled peptides (FOva and TROva), we followed the simultaneous dissociation and reassociation of peptide. In extension of the dissociation experiments, we incubated I-A^d for 10 days with an excess of TROva-(323–339)Y as described before. Afterwards, the I-A^d heterodimer was isolated from the excess of unbound peptide by HPSEC. Again, monitoring of peptide dissociation was started immediately by splitting the samples and adding FOva peptide and buffer to a final concentration of 0.3 μM I-A^d/100 μM FOva-(323–339)/1 mM DM/10 mM phosphate or acetate buffer, pH 7.0 or 5.0/150 mM NaCl/0.02% NaN_3. By injecting small sample volumes into the HPSEC at various times, we could follow peptide association and dissociation. The data for the dissociation are shown in Fig. 2. The association and exchange of the differently labeled peptide was slow (Fig. 3*A*). The data for the peptide exchange fit a pseudo-first-order binding (Fig. 3*B*). The rate constant was $k = 5.8 \times 10^{-6}$, which correlates with the dissociation rate constant found in the same experiment (Fig. 2). Furthermore, we investigated the peptide exchange at different peptide concentrations. Again, we found that the exchange rate was independent of the peptide concentration: the association rate constant for 50 μM FOva peptide was $6.6 \times 10^{-6}\ s^{-1}$ compared to $5.8 \times 10^{-6}\ s^{-1}$ for 100 μM FOva peptide. We investigated the association of a truncated peptide to the preformed MHC–peptide complex. FOva-(323–328) associated specifically and with the same rate constant as the dissociation of prebound peptide ($k = 6.7 \times 10^{-6}\ s^{-1}$). The amount of bound truncated peptide was about a factor of 5 less. In all experiments the kinetic data were independent of the fluorescent dye that was used for peptide labeling. Furthermore, the kinetic data are consistent with experiments using only the dissociation or association of peptide with only one labeled peptide.

Peptide Exchange at Lower pH. The peptide exchange experiments were also conducted at pH 5.0. Corresponding to an increase of the dissociation rate at pH 5.0, both the amount and the rate of association were increased at the beginning of the experiment. The amount of bound peptide reached a maximum at 15 hr and diminished thereafter. In another experiment the amount of peptide associated with I-A^d was determined at various pH values. After incubation for 5 days with 100 μM FOva-(323–339)Y the samples were analyzed by HPSEC and SDS/PAGE. The lanes containing samples that were incubated at different pH values were

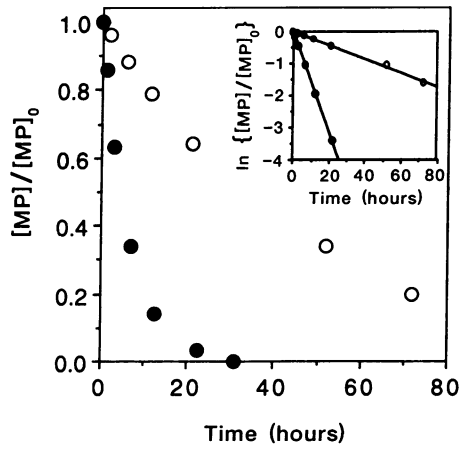

FIG. 2. Dissociation of the MHC–peptide complex. After incubation of I-A^d for 10 days with an excess of TROva-(323–339)Y in a small sample volume, the I-A^d–peptide complex was isolated by HPSEC. To prevent dissociation the sample was held at 4°C. The dissociation reaction was immediately started at 37°C by splitting the sample and adding an excess of differently labeled peptide and buffer to give 0.3 μM I-A^d/100 μM FOva-(323–339)Y/10 mM phosphate or acetate buffer, pH 7.0 or pH 5.0/150 mM NaCl/0.02% NaN_3. At various times the dissociation of peptide was analyzed by injection of a small volume onto the HPSEC column. At the size-exclusion volume of the heterodimer the fluorescence intensity of peptide bound to I-A^d was determined. $[MP]/[MP]_0$ is given as function of time at pH 7.0 (○) or pH 5.0 (●), where $[MP]_0$ is the initial concentration of bound peptide. (*Inset*) Corresponding to a first-order dissociation, $\ln\{[MP]/[MP]_0\}$ is given as a function of time.

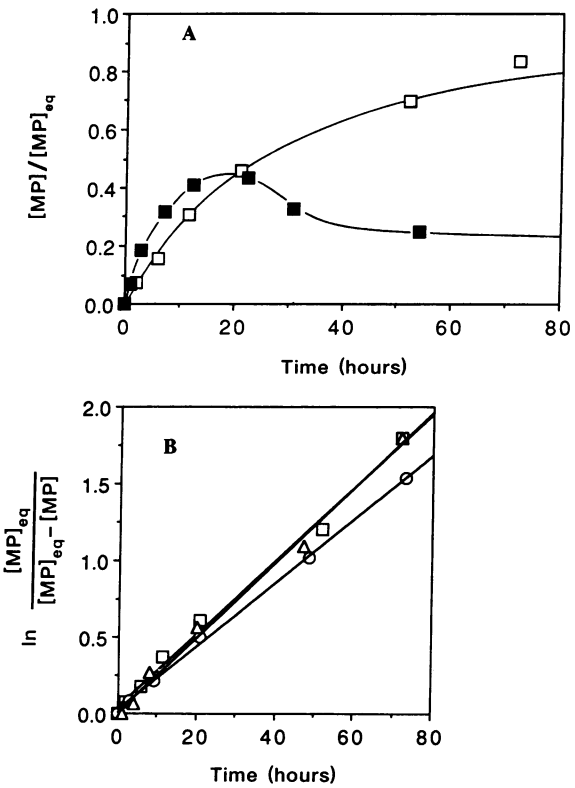

FIG. 3. Exchange of FOva-(323–339)Y to a preformed I-A–TROva-(323–339)Y complex. The association of the FOva peptide was followed simultaneously with the dissociation, as shown in Fig. 2. The samples (0.3 μM I-A^d/50 μM FOva peptide) were incubated at 37°C. At various times peptide exchange was analyzed by HPSEC of a small sample. At the size-exclusion volume of the heterodimer the fluorescence intensity of peptide bound to I-A^d was determined with the fluorescence spectrometer. (*A*) $[MP]/[MP]_{eq}$ is plotted as a function of time at pH 7.0 (○) or pH 5.0 (●). The data at pH 5.0 were normalized by the same $[MP]_{eq}$ value as for pH 7.0. (*B*) Association and exchange of peptide was investigated using various peptide concentrations or a truncated peptide. For a first-order reaction, $\ln\{[MP]_{eq}/([MP]_{eq} - [MP])\}$ is shown as a function of time. ○, 50 μM FOva-(323–339)Y; □, 100 μM FOva-(323–339)Y; △, 100 μM FOva-(323–328).

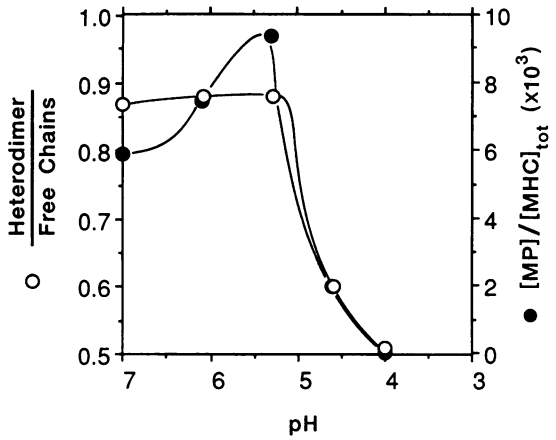

FIG. 4. Stability and peptide binding at various pH values. Lanes of a silver-stained SDS/polyacrylamide gel were analyzed by laser scanning. Samples (0.3 μM I-A^d/100 μM FOva-(323–339)Y/1 mM DM/10 mM phosphate/citrate buffer (pH 7.0–4.0)/150 mM NaCl/0.02% NaN_3) were incubated for 5 days at various pH values at 37°C. A sample (20 μl) was applied to an SDS/12.5% polyacrylamide gel. ○, Ratio of the amount of α/β heterodimer to free α and β chains; ●, amount of peptide bound to the heterodimer, $[MP]/[MHC]_{tot}$, as determined by HPSEC.

silver-stained and analyzed by laser scanning. The ratio of the amounts of heterodimer to free chains was determined (Fig. 4). Below pH 5.3 the amount of heterodimer was drastically decreased. The heterodimer dissociated into free chains. In the same samples the amount of IA^d-bound peptide was determined by HPSEC. Peptide binding increased as the pH was decreased from 7.0 to 5.3 (Fig. 4). The relative amount of bound peptide reached a maximum at pH 5.3. Paralleling the instability of the heterodimer below pH 5.3, the absolute amount of bound peptide also diminished.

DISCUSSION

The half-time for binding of fluorescently labeled Ova-(323–338)Y peptide with MHC class II molecules is independent of the peptide concentration in the range 5–200 μM. In all experiments at pH 7.0 the pseudo-first-order rate constant was determined to be $\approx 1 \times 10^{-5}$ s^{-1} (Fig. 1*C*). Thus, the association of antigenic peptide with MHC class II molecules is not a single-step, second-order association reaction as assumed by other authors (6, 7).

The simplest, qualitative explanation of our results is given by kinetic model I.

$$MP_1 \rightleftharpoons M + P_1 \qquad [1]$$

$$M + P_2 \rightleftharpoons MP_2 \qquad [2]$$

In this model the dissociation of the first peptide, P_1, is the rate-limiting, slow reaction step producing empty MHC molecules, M, that then bind the second peptide, P_2. Our experimental data can be approximated with this model (Fig. 5). In these calculations, the off-rate for reaction **1** is measured directly, and the bimolecular on-rate for reaction **2** is determined from the off-rate for reaction **1** and the equilibrium constant. The equilibrium constant is determined from the long-time asymptotic values of the fluorescent complex concentration as a function of added fluorescent peptide concentration. There are two significant reservations that must be made concerning the comparison between experiment and calculations based on model I. (*i*) Detailed calculations show that, especially at the lower added peptide concentrations, the binding curve is not simply exponential but is sigmoidal, giving rise to a time lag in binding (see Fig. 5). This is the time delay between P_1 dissociation and P_2 binding. This lag is not seen experimentally. However, calculations show that the time lag would not be seen if a small proportion ($\approx$10%) of the MHC molecules were uncomplexed at the beginning of the experiment. (*ii*) A more serious discrepancy is that even after extensive dialysis, the half-time for peptide binding is found to be equal to the half-time for fluorescent peptide dissociation. The extensive dialysis should give empty MHC molecules, and in model I these should show a peptide-concentration-dependent half-time for peptide binding. We have never observed this experimentally. But again there is a caveat: MHC molecules with empty binding sites may denature slowly.

Model II assumes a kinetic intermediate. More narrowly, the MHC molecule can have two conformations, "open" and "closed," M_o and M_c.

$$M_o + P \rightleftharpoons M_oP \qquad K = [M_o][P]/[M_oP] \qquad [3]$$

$$M_oP \rightleftharpoons M_cP \qquad [4]$$

Let reaction **3** be fast and reversible, and let reaction **4** be slow and reversible. When reaction **3** is sufficiently fast, the formation and dissociation of M_cP are each described by a single exponential. Calculations show that under a range of conditions, model II is consistent with the experimental data in that the half-time for peptide binding can be comparable to the half-time for peptide dissociation, for a sizable range of added peptide concentrations. For example, when the free peptide concentration is essentially constant, either because it is large compared to the MHC concentration (or very small), then the half-time for the binding (or dissociation) reaction is

$$t_{1/2} = [k_{co} + ([P_o]k_{oc})/([P_o] + K)]^{-1}(\ln 2). \qquad [5]$$

Here k_{oc} and k_{co} are the first-order rate constants for the forward and reverse reactions **4**. In the binding reaction, $[P_o]$ is the concentration of added peptide; for the dissociation

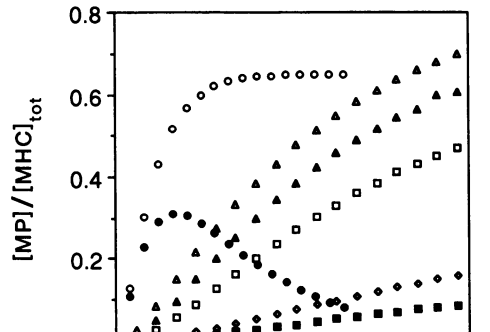

FIG. 5. Simulation of peptide exchange by kinetic model I:

$$MP_1 \xrightarrow{k_1} M + P_1$$

$$M + P_2 \underset{k_4}{\overset{k_3}{\rightleftharpoons}} MP_2 \quad (k_4/k_3 = K_d)$$

$$M \xrightarrow{k_5} 0$$

For simulation we solved two differential equations, $d[M]/dt = k_1[M]_{tot}\exp(-k_1t) - k_3[M]([P] - [MP_2]) + k_4[MP_2] - k_5[M]$ and $d[MP_2]/dt = k_3[M]([P] - [MP_2]) - k_4[MP_2]$, with the following experimental data. For pH 7.0, $k_1 = k_4 = 10^{-5}$ s^{-1}, $K_d = 28$ μM, $k_5 = 0$ s^{-1}: △, [P] = 200 μM; ▲, [P] = 100 μM; □, [P] = 50 μM; ◇, [P] = 10 μM; ■, [P] = 5 μM. For pH 5.0, $k_1 = k_4 = 4 \times 10^{-5}$ s^{-1}, $K_d = 28$ μM, $k_5 = 4 \times 10^{-5}$ s^{-1}: ●, [P] = 50 μM; ○, [P] = 50 μM but with $k_5 = 0$.

reaction, use $[P_o] = 0$. There are substantial ranges of parameter space where the two half-times are of the same magnitude. For example, if k_{co} and k_{oc} are equal, then the binding and dissociation half-times never differ by more than a factor of 2, no matter what the peptide concentration. However, in general there is some dependence of half-time on peptide concentration, according to Eq. 5. For illustrative kinetic parameters, see ref. 8.

We have considered the possibility that the data in Fig. 1*B* do not represent equilibrium, but rather a steady state, resulting from dissociation of endogeneous peptide, followed by a competition between the binding of added peptide and denaturation of the MHC molecule. This model leads to a steady-state concentration of bound fluorescent peptide that is proportional to the added peptide concentration, a result at variance with the data in Fig. 1*B*.

Model III embodies features of model I and model II together with the above assumption that emply MHC molecules "die"—that is, they irreversibly denature or are otherwise removed from the system. In model III the kinetic intermediate has two bound peptides, X and P.

$$MX + P \rightleftharpoons MXP \quad [6]$$

$$MXP \rightleftharpoons MPX \quad [7]$$

$$MPX \rightleftharpoons MP + X \quad [8]$$

In this scheme reactions **6** and **8** are rapid and reversible, reaction **7** is slow and reversible, and the dissociation reaction, **1**, leads to irreversible loss of the MHC molecule. Reaction **7** has an equilibrium constant of about 1, and reactions **6** and **8** have, for example, micromolar equilibrium constants. With these reactions it will be seen that one can mimic the kinetic binding curves in Fig. 1 *A* and *B* and can account for the fact that the half-time for binding to form MP is approximately equal to the half-time for peptide dissociation, providing this is equal to the half-time for reaction **7**.

The long half-time for reaction **4** or **7** may depend largely on structural features of the MHC molecule, and less so on the peptide itself. This is suggested by the observation (Fig. 2*B*) FOva(323–339)Y as well the truncated peptide FOva(323–328) bind with the same half-time. In comparing calculations based on model II (III) with experiment we have assumed that M_oP (MXP or MPX) dissociates during HPLC, whereas M_cP (MP) remains intact and is detected and measured as "fluorescent complex." This assumption is consistent with the earlier study of a kinetic intermediate involving I-E^k and pigeon cytochrome *c* in planar lipid membranes (8). Further fluorescence experiments using planar membranes, or other techniques, will be necessary to obtain accurate data on kinetic intermediates of I-A^d–Ova peptide complexes.

The acidification of endosomal compartments is an important factor in antigen processing and presentation. Lysosomotropic agents (e.g., chloroquine and NH_4Cl) disrupt intracellular pH gradients and inhibit processing and presentation of antigen (11). Recently, Jensen (12) demonstrated that preincubation of fixed antigen-presenting cell surfaces with peptides at low pH causes an increased stimulation of T helper cells. For this reason we investigated the association and exchange of peptide at different pH values. At pH 5.0 the dissociation rate is increased by a factor of 7. Corresponding to this observation, both the rate of binding and the amount bound are increased at early times, <10 hr. The amount of α/β heterodimer–peptide complex reaches a maximum and diminishes thereafter. The heterodimer dissociates into free α and β chains. At long times, >10 hr, the amount of α/β heterodimer–peptide complex is greatly reduced (Fig. 4). Fig. 5 shows how inclusion of a finite lifetime in model I can account for data such as those at low pH where there is a loss of MHC heterodimers. The estimated half-time for dissociation into α and β chains is 7 hr. This effect can easily be included in model II or III. The dissociation of the heterodimers into subunits at pH 5.0 is sufficiently slow that it may play no significant role in molecular events in the endosomal compartments. It remains to be seen how these results relate to the previously described "floppy" conformation of class II MHC molecules (13) and whether they are generically related to the reported instability of empty class I molecules (14).

We thank Dr. Brian Clark for the help in the peptide synthesis. This work was supported by the Max-Kade Foundation (R.T.) and National Institutes of Health Grant 5R01 AI13587-13.

1. Unanue, E. (1984) *Annu. Rev. Immunol.* **2,** 395–428.
2. Buus, S., Sette, A. & Grey, H. M. (1987) *Immunol. Rev.* **98,** 115–141.
3. Harding, C. V. & Unanue, E. R. (1989) *J. Immunol.* **142,** 12–19.
4. Babbitt, B., Allen, P. M., Matseuda, G., Haber, E. & Unanue, E. R. (1985) *Nature (London)* **317,** 359–361.
5. Buus, S., Colon, S., Smith, C., Feed, J. H., Miles, C. & Grey, H. M. (1986) *Proc. Natl. Acad. Sci. USA* **83,** 3968–3971.
6. Buus, S., Sette, A., Colon, S. M., Jenis, D. M. & Grey, H. M. (1986) *Cell* **47,** 1071–1077.
7. Roche, P. A. & Cresswell, P. (1990) *J. Immunol.* **144,** 1849–1856.
8. Sadegh-Nasseri, S. & McConnell, H. M. (1989) *Nature (London)* **338,** 274–276.
9. Kim, K. J., Kanellopoulos-Langevin, C., Merwin, R. M., Sachs, D. H. & Asofsky, R. (1979) *J. Immunol.* **122,** 549–554.
10. Heukeshoven, J. & Dernick, R. (1985) *Electrophoresis* **6,** 103–112.
11. Ziegler, H. K. & Unanue, E. R. (1982) *Proc. Natl. Acad. Sci. USA* **79,** 175–178.
12. Jensen, P. E. (1990) *J. Exp. Med.* **171,** 1779–1784.
13. Rothenhäusler, B., Dornmair, K. & McConnell, H. M. (1990) *Proc. Natl. Acad. Sci. USA* **87,** 352–354.
14. Townsend, A., Öhlen, C., Bastin, J., Ljunggren, H.-G., Foster, L. & Kärre, K. (1989) *Nature (London)* **340,** 443–448.